J Mol Model (2005) 11: 80–86
DOI 10.1007/s00894-004-0229-2

ORIGINAL PAPER

Zhanli Wang · Liangren Zhang · Jingfen Lu
Lihe Zhang

Analysis of the interactions of ribonuclease inhibitor with kanamycin

Received: 12 September 2004 / Accepted: 25 November 2004 / Published online: 12 January 2005

Abstract The interaction of ribonuclease inhibitor (RI) with kanamycin was studied by molecular modeling. The preliminary binding model was constructed using the Affinity module of the Insight II molecular modeling program and the key residues involved in the combination of RI binding to kanamycin were determined. Meanwhile, we determined relevant surface characteristics determining the interaction behavior. The modeling results indicated that electrostatic interactions and H-bond forces may work as major factors for the molecular interaction between kanamycin and RI. The above results are useful for elucidating the molecular principles upon which the selectivity of a kanamycin is based. The quartz-crystal microbalance (QCM) is a new method usually used to monitor the binding function of macromolecules with samples online in a flow-injection analysis (FIA) system. The experimental results demonstrate that kanamycin has an extraordinary affinity to the basic protein RI, and our result is consistent with the molecular modeling results. These principles can in turn be used to study the molecular recognition mechanism and design a mimic of kanamycin for the development of new RI binders.

Keywords Ribonucleases inhibitor (RI) · Kanamycin · Docking · Quartz crystal microbalance (QCM)

Abbreviations RI: Ribonuclease inhibitor · QCM: Quartz crystal microbalance

Z. Wang · L. Zhang · J. Lu (✉) · L. Zhang
State Key Laboratory of Natural and Biomimetic Drugs,
Health Science Center of Peking University,
100083 Beijing, People's Rebublic of China
E-mail: zdsljf@bjmu.edu.cn
Tel.: +86-10-82801517
Fax: +86-10-82802724

Introduction

Mammalian cells contain a potent cytosolic RNase inhibitor (RI), which is a 50-kDa leucine-rich-repeat protein. RI has an extraordinary affinity with ribonucleases of the pancreatic ribonuclease superfamily in a 1:1 stoichiometry [1, 2]. The molecular basis for this high affinity and specificity have been explored by X-ray crystallography and site-directed mutagenesis. A crystal structure has been determined for the complexes of porcine RI with bovine pancreatic RNase A. It is revealed that RNase A bi\nds to the concave region of the inhibitor comprising its parallel β-sheet and loops, and the dissociation constants extend from 10^{-13} to below 10^{-15} mol/l [3]. The interaction is predominantly electrostatic, with the binding likely resulting from direct association of basic proteins with the acidic inhibitor. [4, 5] It has also been proved that highly basic proteins including the homopolypeptides such as Poly -arginine, poly-lysine and poly-ornithine, spermatic-specific S1 protein and the protamine HP3 and Z3 also bind strongly to RI [6].

Kanamycin has long been used as a very efficient drug against Gram-positive and Gram-negative bacteria, and against mycobacterial infections. This molecule is a multiply charged compound of high flexibility. The positive charges of kanamycin are attracted to the negatively charged RNA backbone. The flexibility of the aminoglycosides facilitates accommodaivelyction into a binding pocket within internal loops of RNA helices or into ribozyme cores for making specific contacts. The current studies showed that they preferentially bind to a variety of unrelated RNAs, including prokaryotic ribosomal RNA [7], the TAR [8] and RRE HIV-1 RNA motif [9], several ribozymes and human rRNAs [10].

We hypothesise that the above basic proteins and kanamycin share this common binding strategy and kanamycin may interact with RI. Therefore, in the present investigation, a docking simulation of the RI-kanamycin complex was performed using the Affinity

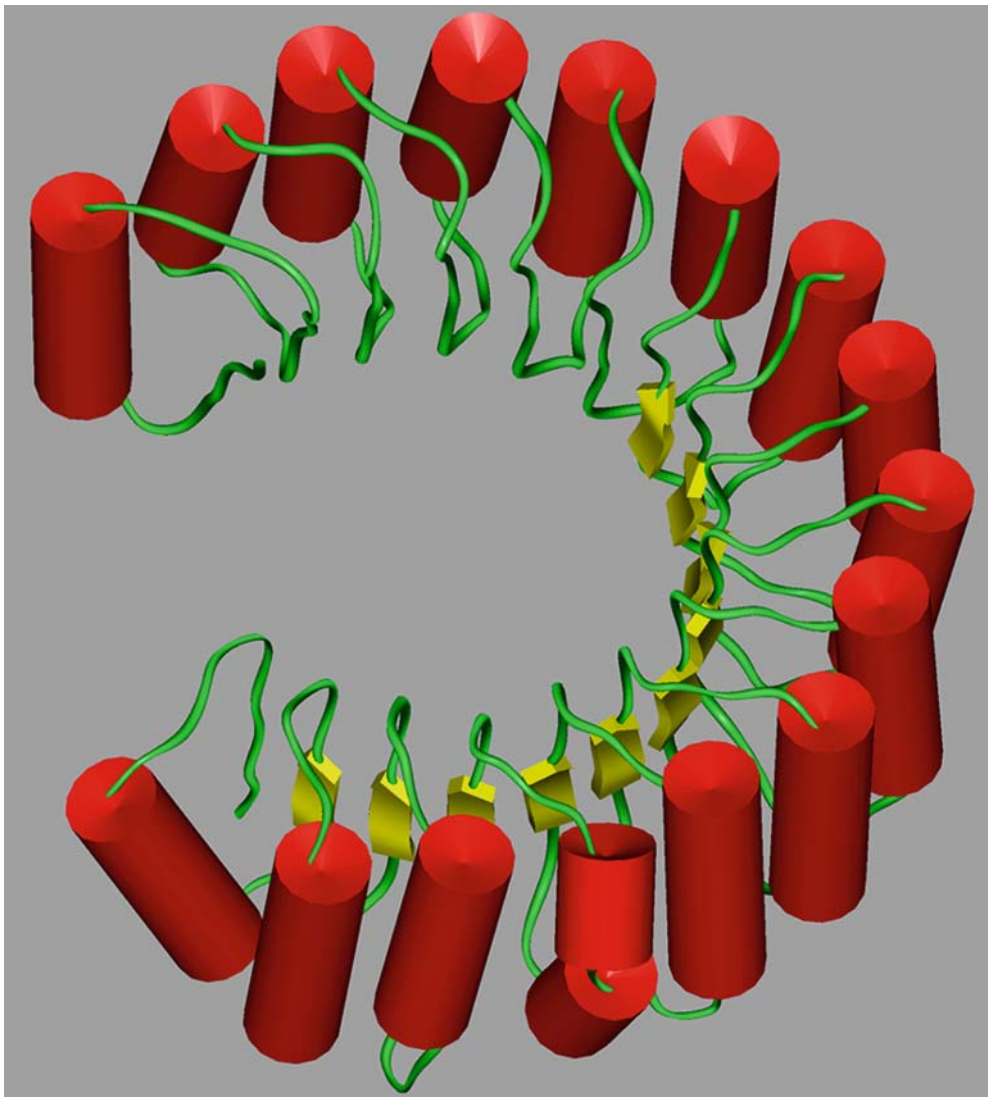

Fig. 1 The 3Dstructure of RI. The α-helix is represented by *red* color and the β-sheet is represented by *yellow* color

module and relevant surface characteristics of RI were determined with the Delphi module. Meanwhile, the Binding constant of the kanamycin–RI complex was measured by the QCM method. Information on the binding domain of RI is important for explaining the binding mechanism of RI and kanamycin and can further help us to design the selective binders of RI.

Materials and methods

Materials

Kanamycin and DL-dithiothreitol (DTT) were purchased from Sigma. Porcine ribonuclease inhibitor (RI) was from Promega. Ethanedioldiglycidyl ether and sodium borohydride were from Sigma (st. Louis, mo, USA). Amount of 100 mmol/l glycine-HCl solution (pH 2.0) was used as regeneration reagent. Unless specially noted, all the solutions of the reagents were in 10 mmol/l phosphate buffered solution (PBS), pH 7.4. All the chemicals used were of analytical grade. Prior to use, all solutions prepared were filter (0.22 μm).

Molecular modeling

All molecular modeling studies were performed on a Silicon Graphics O2 computer running the Insight II software developed by Accelrys, San Diego. The 3D structure of kanamycin was constructed and optimized with the Builder and Discover modules, respectively. Energy minimization was performed using standard steepest descent and conjugated gradient minimization algorithms implemented in the program. For tracking the interaction mode of RI with kanamycin, a computational docking study was performed based on the reported RI structure (pdb code, 2BNH) [11]. The advanced docking program Affinity was used for the automated molecular docking. The best binding struc-

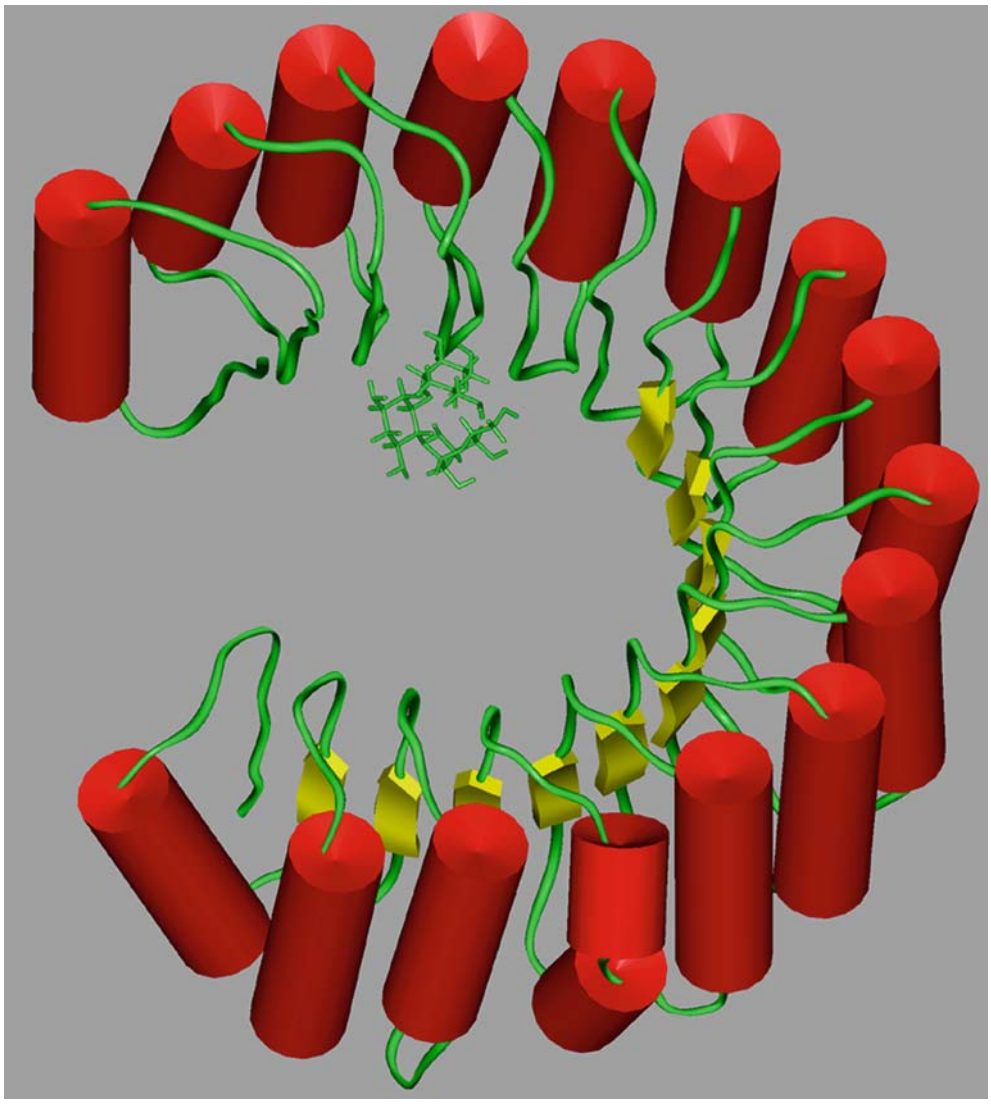

Fig. 2 Proposed binding model of kanamycin to *RI* obtained by the computer-aided docking method and optimized with molecular mechanics with the CVFF forcefield

ture of the ligand to the receptor based on the energy of the ligand/receptor complex was found automatically by Affinity. The consistent valence forcefield (CVFF) was selected prior to perform docking calculations and the cell-multipole approach was used for nonbond interactions [12]. To account for the solvent effect, the centered RI–kanamycin complexes are solvated in a sphere of TIP3P water molecules with radius 10 Å. The initial position of kanamycin within the RI binding site was found using a Monte Carlo type procedure to search both conformational and Cartesian space. If the resulting ligand/receptor system was within a predefined energy tolerance of the previous structure, the system was subjected to minimization. The resulting structure was accepted on the basis of an energy check. Second, a simulated-annealing phase optimized ligand placement and the structures were then subjected to energy minimization based on molecular dynamics. The final conformations were obtained through a simulated-annealing procedure from 500 to 300 K, and then 5000 rounds of energy minimization were performed to reach convergence.

To further elucidate RI-kanamycin interaction, surface properties of RI were investigated using the Delphi module of the Insight II molecular modeling program. Delphi is a program for calculating electrostatic properties, including the effects of bulk solvent and ionic strength, thereby providing crucial data for the specificity of ligand–receptor interactions.

Real-time analysis of the binding of RI to kanamycin with QCM

The binding of RI to immobilized kanamycin was measured using the QCM-FIA system following the previously described procedure [13]. Briefly, kanamycin was immobilized on a piezoelectric crystal followed by treatment with ethanolamine hydrochloride (pH 8.6, 1 mol/l water solution) for 30 min, the fresh kanamycin-

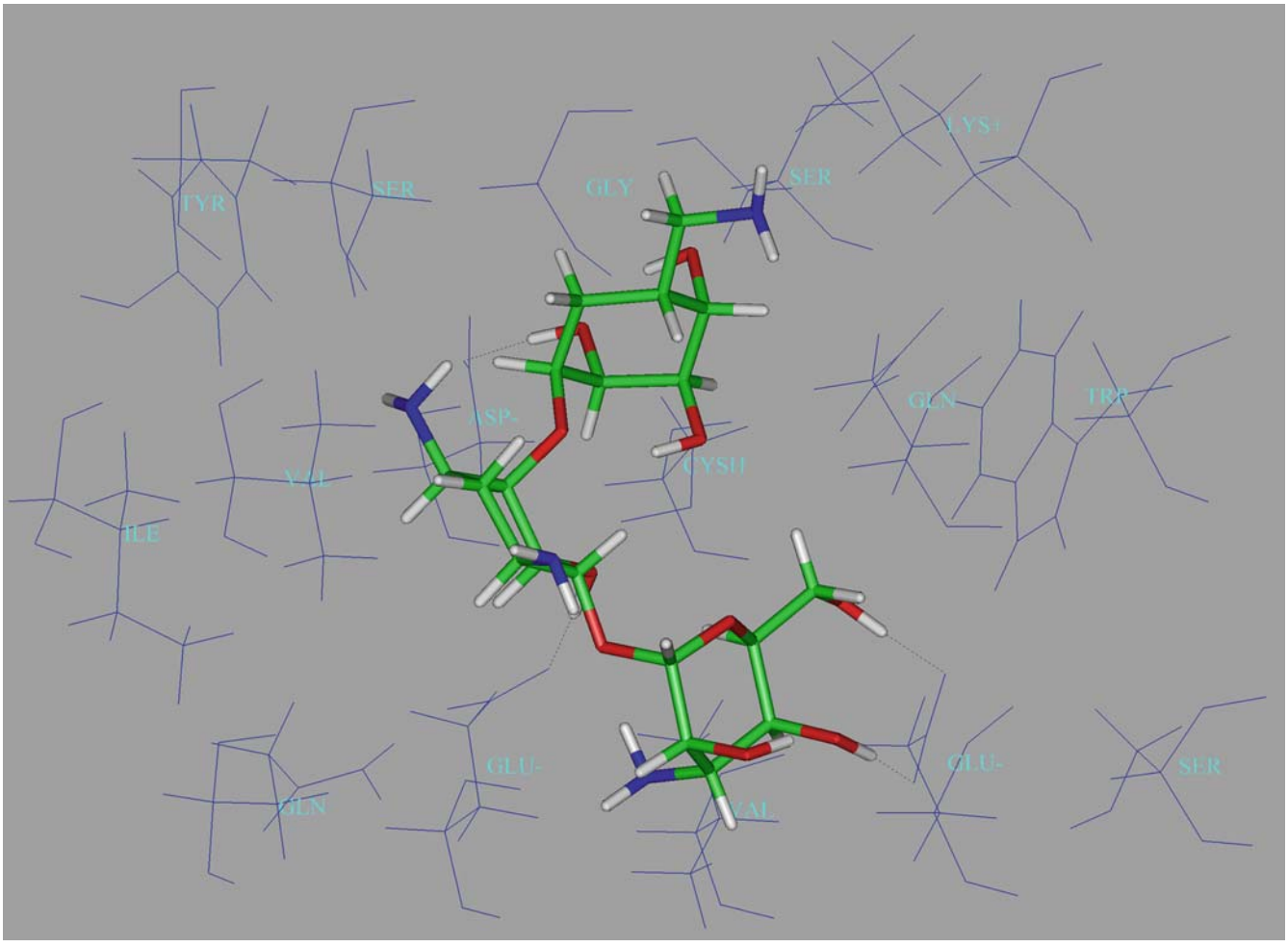

Fig. 3 Interaction between kanamycin and RI as predicted by molecular modeling. The hydrogen bonds are labeled by *black lines*

coated quartz crystal was mounted in the flow-through system and rinsed with PBS (pH 7.4, 10 mmol/l) continuously until the frequency stabilized under the flow conditions (60 μl/min). The crystal was powered by an oscillator, which was constructed by a transistor–transistor logic integrated circuit (TTL-IC). By means of an injection valve, 200 μl aliquots of various concentrations of RI solutions were injected into the fluid system. The curves of permanent frequency shifts versus. time were recorded and the binding process was monitored in real time. The frequency output was recorded with an EE3386 Universal Counter (Nanjing Telecommunication Instrumental Factory, Nanjing, China) controlled by a personal computer via the RS 232 interface. After one binding measurement, 600 μl glycine-HCl solutions (100 mmol/l, pH 2.0) were injected into the system through an injection valve to dissociate the bound biomolecules and regenerate the surface of the electrode for the next binding. All binding experiments were carried out at room temperature at a constant flow rate of 60 μl/min of buffer.

Results and discussion

Figure 1 shows the 3-D structure of RI, a cytoplasm proteins that binds alkaline ribonucleases A tightly and inhibits them by providing an extensive binding area for the RNase A [1, 2]. RNase A is a positively charged molecule that establishes polar contacts with the concave region of its surface and electrostatic interactions are critical for binding [14, 15]. In order to simulate the interaction between the RI and kanamycin, molecular

Table 1 The docking energy between kanamycin and RI

Intermolecular energy (kcal mol^{-1})			Molecular energy (kcal mol^{-1})			
Vdw	Elect	Total	Vdw-repulsive	Vdw-dispersive	Elect	Total
−8.35	−101.74	−110.09	1121.99	−1045.70	−363.65	−287.36

Table 2 H-bond between kanamycin and residues in the binding sites

RI (Receptor)	Kanamycin (Ligand)	Distance (Å)
GLU-397: OE2	H22	1.39
ASP-399: OD1	H19	1.37
GLU-340: OE1	H21	1.42
GLU-340: OE2	H20	1.41

modeling calculations were carried out to study the interaction under the assumption that kanamycin and ribonucleases A interact at similar receptor binding sites. To construct a binding model of kanamycin and the binding site of RI, a computational docking study was performed based on the reported RI structure. Figure 2 shows a possible energy-minimized docking model of kanamycin and RI. In this model, we can see that the binding site is in general depressions in the protein surface and kanamycin locates in the center of the binding pocket. The binding site includes Glu340, Gln342, CYSH371, Glu397, Asp399 and Gln 426 (Fig. 3). Most of these amino acid residues are acidic, and most of them play an essential role for ribonucleases–RI interaction. The experimental results suggest that this kind of binding is similar to the ribonucleases. The docking studies were reproducable when repeated, and other possible interaction sites were not observed within the docking experiments, which were evaluated using the interaction energy function.

The modeling studies investigated the conformational and electrostatic properties of the receptor and

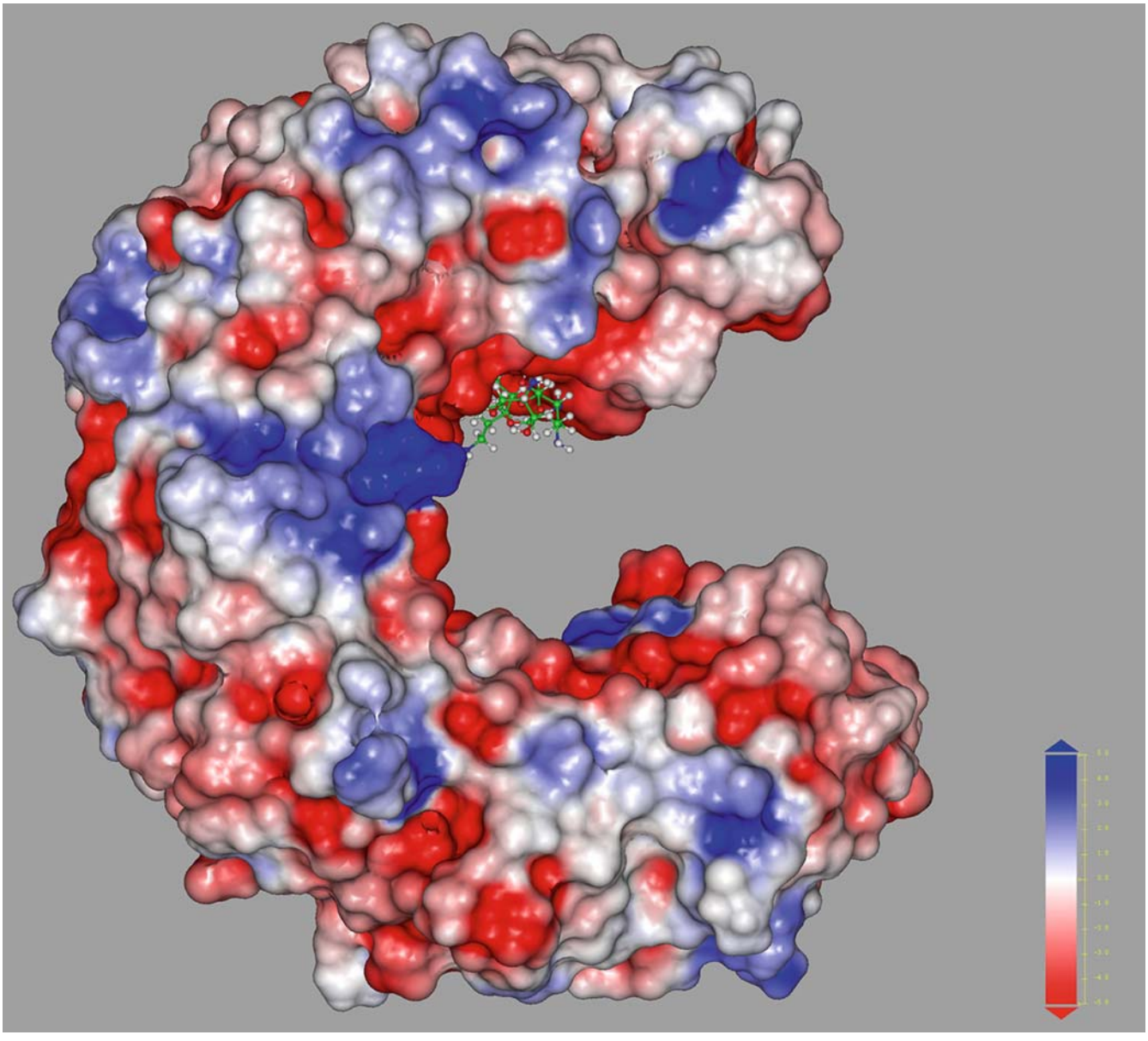

Fig. 4 A 3D complex sructure of RI-kanamycin obtained by computer-aided docking method. *RI* is represented as a molecular surface colored by electrostatic potential

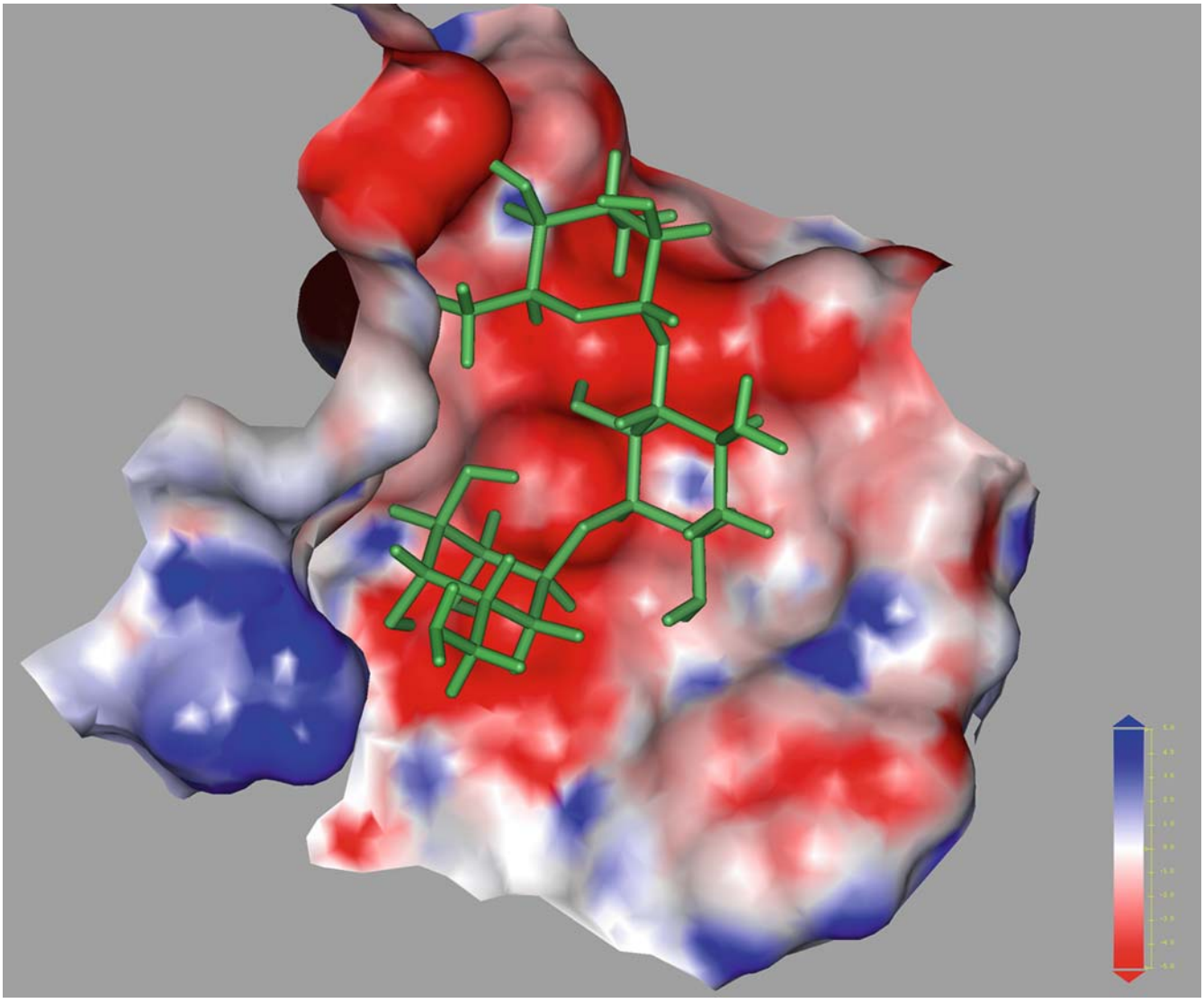

Fig. 5 A 3D structure of kanamycin in RI binding groove. *RI binding groove* is represented as a molecular surface colored by electrostatic potential

ligand in order to understand the molecular mechanism of the binding of kanamycin to RI. Table 1 gives the molecular energy and intermolecular energy including the total, van der Waals and electrostatic energies. This table shows that there is a large favorable total interaction energy for the RI–kanamycin and the total intermolecular energy is -110.09 kcal mol^{-1}. The van der Waals and electrostatic energies are -8.35 and -101.74 kcal mol^{-1}, respectively. This means that one important character of the interaction between RI and kanamycin is the electrostatic interaction. The major contribution of the van der Waals repulsion to the barrier can be traced back to the steric and hydrophobic interactions near the binding domains of RI. From Table 2 we know that several hydrogen bonds are formed between kanamycin and some residues of RI. These interactions lead to a large stabilization of kanamycin in this region.

Table 3 Computed SAS of amino acids in binding sites

	SAS area (Å^2)	Polar (Å^2)	Nonpolar (Å^2)
Glu340	56.635	45.298	11.337
Gln342	26.926	23.762	3.164
CYSH371	19.313	16.418	2.895
Glu397	35.533	27.553	7.98
Asp399	19.511	17.279	2.233
Gln426	48.235	45.114	3.122

Together with the energetic docking approach, which studies the binding sites on the molecular surface of proteins according to the binding energy (including electrostatic, non electrostatic and hydrogen bonding), surface properties have played a significant role in protein docking research. Delphi calculates electrostatic solvation properties for molecules. This flexibility allowed us to examine entire receptor–ligand interactions. In this paper, the Connolly molecular surface was calculated using the Delphi module of the Insight II

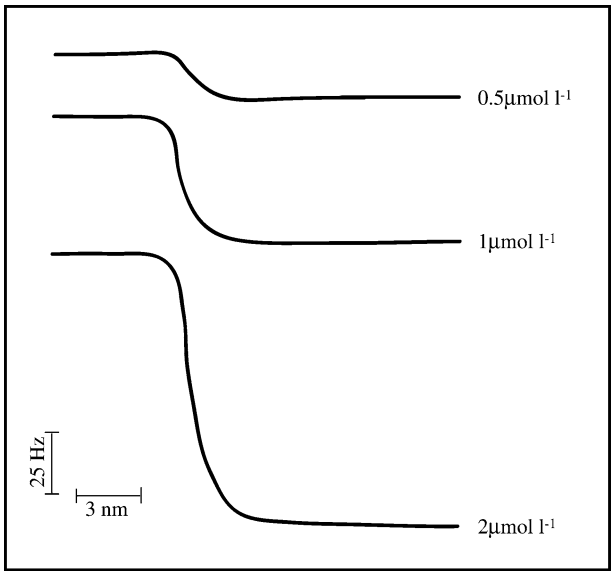

Fig. 6 The individual binding curves for several concentrations of RI with immobilized kanamycin

Table 4 The kinetic and equilibrium constants characterizing affinity interaction of RI with immobilized kanamycin

Kass	Kdiss	KA
2591.7 mol^{-1} s^{-1}	2.28×10^{-3} s^{-1}	1.14×10^{6} M^{-1}

molecular modeling program. The surface is color coded by electrostatic potential as shown in Figs. 4 and 5. The spectrum shows that negative and positive regions are opaque red and blue, respectively. The solvent-accessible surface of RI with the bound kanamycin, shows the electrostatic potential energy values calculated for the binding site of RI. The center area is strongly negatively charged (red), surrounded by an area of neutral charge (white), and areas of positive charge (blue). These simulations revealed that the overall charge of the binding site makes an important contribution to the binding of molecules. To determine the key residues that comprise the binding pocket of the model, the solvent accessible surface (SAS) of each individual amino acid in the binding site was also calculated. This identification, compared with a definition based on the distance from the ligand, can clearly show the relative significance for every residue. Table 3 gives the areas of solvent-accessible surface including the polar and nonpolar areas. From Table 3 we know that the residues Glu340, Gln342, CYSH371, Glu397, Asp399 and Gln426 have similar behavior and the interaction of these residues with kanamycin consist mainly of the electrostatic interaction.

From the real-time analysis by the QCM experiment, specific binding of kanamycin with RI was observed. It was shown in Fig. 6 that when 200 μl of RI solution was injected into the cell, the frequency decreased significantly. On rinsing with the buffer solution, the frequency did not return to the initial baseline. This result confirmed clearly that the specific interaction between RI and kanamycin takes place under these conditions. The effects induced by various concentrations of RI on the association with immobilized kanamycin were measured and recorded as sensorgrams (Fig. 6). It is shown that the interaction is concentration dependent. A standard assay was used for determining the binding constants [13]. The association and dissociation of various concentrations of RI with the immobilized kanamycin were recorded as sensorgrams. The sensorgram data were analyzed using our in-house kinetic analysis software based on a GA running on a PC with a Pentium III processor to obtain precise information of the kinetic rate constants. The results of kinetic and equilibrium constants for RI were summarized in Table 4. The results reveal a moderate association rate constant (2591.7 mol^{-1} s^{-1}) and a low dissociation rate constant (2.28×10^{-3} s^{-1}) resulting in a relatively high binding affinity (1.14×10^{6} M^{-1}).

Acknowledgment We thank the National Natural Science Foundation of China for financial support (NSFC 20132030, 20332010).

References

1. Lee FS, Vallee BL (1993) Prog Nucleic Acid Res Mol Biol 44:1–30
2. Kobe B, Deisenhofer J (1995) Nature 374:183–186
3. Vicentini AM, Kieffer B, Matthies R, Meyhack B, Hemmings BA, Stone SR, Hofsteenge J (1990) Biochemistry 29:8827–8834
4. Moenner M, Hatzi E, Badet J (1997) In Vitro Cell Dev Biol—Anim 33:553–561
5. Papageorgiou AC, Shapiro R, Acharya KR (1997) EMBOJ 16:5162–5177
6. Moenner M, Chauvière M, Chevaillier P, Badet J (1999) FEBS Lett 443:303–307
7. Moazed D, Noller HF (1987) Nature 327:389–394
8. Mei H-Y, Galan AA, Halim NS, Mack DP, Moreland DW, Sanders KB, Troung HN, Czarnik AW (1995) Bioorg Med Chem Lett 5:2755–2760
9. Zapp ML, Stern S, Green MR (1993) Cell 74:969–978
10. Hamasaki K, Rando RR (1997) Biochemistry 36:12323–12328
11. Kobe B, Deisenhofer J (1993a) Nature 366:751–756
12. Dauber-Osguthorpe P, Roberts VA, Osguthorpe DJ, Woff J, Genest M, Hagler AT (1998) Protein 4:31–47
13. Liu Y, Yu X, Zhao R, Shangguan D-H, Bo ZY, Liu GQ (2003) Biosen Bioelec 19:9–19
14. Kobe B, Deisenhofer J (1996) J Mol Biol 264:1028–1043
15. Makarov AA, Ilinskaya ON (2003) FEBS Lett 540:15–20